



Biogenic zinc oxide, copper oxide and selenium nanoparticles: preparation, characterization and their anti-bacterial activity against *Vibrio parahaemolyticus*

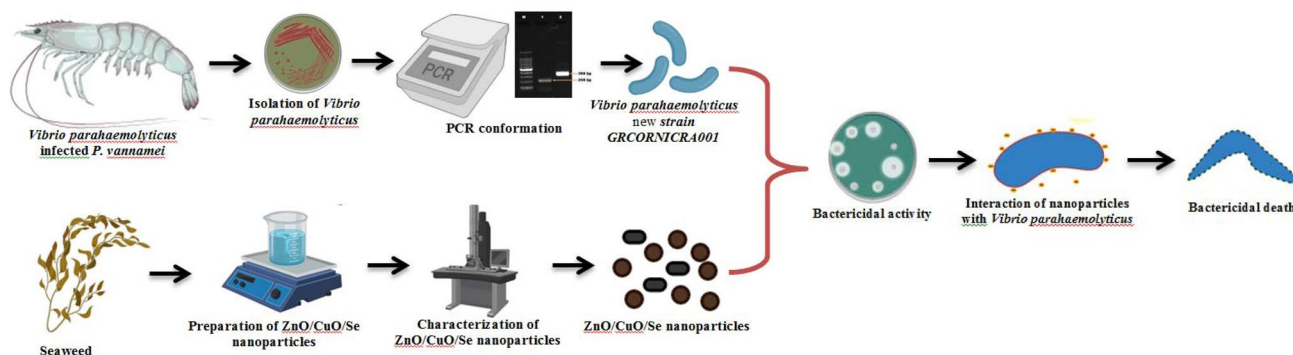
D Vinu¹ · K. Govindaraju¹ · R. Vasantharaja¹ · S. Amreen Nisa¹ · M. Kannan² · K. Vijai Anand³

Received: 5 July 2020 / Accepted: 29 October 2020 / Published online: 12 November 2020
© Islamic Azad University 2020

Abstract

The present study investigates biogenic preparation of zinc oxide (ZnO), copper oxide (CuO) and selenium (Se) nanoparticles using the marine brown alga *Sargassum swartzii*. The prepared nanomaterials were characterized using X-ray diffraction pattern (XRD), scanning electron microscopy (SEM) equipped with energy dispersive X-ray analysis (EDAX), transmission electron microscopy (TEM) and UV–Vis diffuse reflectance spectroscopy (DRS-UV) analysis. The particle size of biogenic ZnO, CuO and Se nanoparticles was ca. 32, 32 and 21 nm, respectively. The isolation of bacterial pathogenic strain *Vibrio parahaemolyticus* (*V. parahaemolyticus*) from the diseased shrimp and virulent genes (*toxR* and *tlh*) confirmed by PCR technique. Further, the molecular characterized using 16S ribosomal RNA gene sequences and identified new strain *V. parahaemolyticus* strain (GRCORNICRA001). Anti-bacterial activity of biogenic nanomaterials (ZnO, CuO and Se) was investigated against isolated *V. parahaemolyticus* using well diffusion method and growth inhibitory assay. The minimum inhibitory concentration (MIC) was 25, 25 and 10 $\mu\text{g mL}^{-1}$ of ZnO, CuO and Se nanoparticles, respectively. The results show that there is a strong bacterial inhibition in a dose-dependent manner. Further, SEM analysis revealed that the interaction of nanomaterials with *V. parahaemolyticus*, resulted in a surface tension change that leads to membrane depolarization, formation of abnormal textures such as membrane rupture, membrane blebs, membrane clumping, and also caused cell death. Results of this effort highlighted the way for the future that these nanomaterials incorporated with shrimp feed for the management of aquatic diseases.

Graphic abstract



Keywords Seaweed · Nanomaterials · 16S ribosomal RNA sequences · Anti-bacterial activity · SEM

Electronic supplementary material The online version of this article (<https://doi.org/10.1007/s40097-020-00365-7>) contains supplementary material, which is available to authorized users.

Extended author information available on the last page of the article

Introduction

Aquaculture is one of the largest food producing sectors across the globe. Disease is considered to be one of the major limiting factors in aquaculture production worldwide. It is witnessed that the aquaculture industry particularly, shrimp culture has been continuously suffered by various diseases that are caused by bacteria and viruses leading to high mortality rate, and huge economic loss [1]. Among pathogens, bacteriae belonging to family Vibrionaceae are the most significant and cause for high mortality rate in shrimp industry worldwide. Currently, newly emerged bacterial disease called early mortality syndrome (EMS) in penaeid shrimps is named as acute hepatopancreatic necrosis disease (AHPND) infected by *Vibrio parahaemolyticus* (*V. parahaemolyticus*) has been reported [2] and caused highest mortality (100%) within the 30 days of culture and led to a major economic losses more than 1 billion US\$ by value in Asia–Pacific region alone [3]. Impacts on aquaculture trades, many countries have banned the import of live shrimps and their products from countries affected by AHPND [4]. Many approaches have been addressed to control vibriosis diseases in shrimp industry, such as water monitoring and replacements, management practices, use of antibiotics; though, in aquaculture industry, there is a hazard by use of antibiotics might lead to resistance in bacteria that threaten not only shrimp but also humans [5, 6]. Hence, alternative materials such as plant extracts, phages, probiotics, immunostimulants, recombinant immune-related proteins, silver nanoparticles have been used for the treatment of AHPND infection [7, 8].

In recent years, metal oxides which exhibit superior remarkable properties such as electronic [9], electrochemical [10], catalytic [11], energy and environment [12], biomedical properties [13] become much important for various potential applications [14]. Among which, ZnO (II-VI) semiconductor with distinctive properties such as wide band-gap, and large exciton binding energy has stimulated much attention and numerous applications such as gas sensors, biosensors, photo-catalyst, solar cells, and anti-bacterial agent [15]. Similarly, copper oxide also provoked much interest due its unique semiconductor, optical and anti-bacterial properties and hence finds potential applications such as biocidal activity, catalysis, and anti-bacterial activity [14, 16]. Nanomaterials with small size and large surface area will improve its bioactivities. Among which, selenium is a well-known structural component of the active center of various antioxidant enzymes and functional proteins. It can contribute in different redox reactions due to its multiple oxidation states. Further, it is an essential trace element for human due to its pro-oxidative, and anti-oxidative effects [17, 18].

Although various chemical and physical protocols are used for the preparation of metal nanoparticles, various green and affordable preparation techniques have been expanded using plants, microbes (bacteria, fungi, yeast etc.) [19–21] and their therapeutic applications such as anti-microbial activity [22, 23], anti-cancer [24, 25], anti-diabetic [26, 27], cardiovascular [28], agricultural applications [29, 30] etc., Among the natural resources, seaweeds (macroalgae) have potent resources use of natural, cost effective, high stability, and bio-compatible materials as stabilizing agents (polysaccharides) in the preparation of metal nanoparticles. Further, these bio-agents are accomplished of providing enough stability in various therapeutic applications even in the presence of electrolytes and under conditions of different pH [31–33].

Nanoscience and technology has a remarkable potential to transform agriculture and allied sector which includes, aquaculture and fisheries [34, 35]. It can provide new tools and techniques for rapid disease diagnosis [36] and to improve the ability of cultivable species to uptake nutrients [37], hormones delivery [38], and vaccines delivery [39]. The trace elements such as, chromium, cobalt, copper, iodine, iron, manganese, molybdenum, selenium, and zinc precursor salts that have been used in the aquafeed involved variety of function that includes cellular metabolism, immune enhancer, various stress releaser, disease resistance, and other physiological functions [40]. The objectives of the present study are four fold: firstly, biogenic preparation and physico-chemical characterization of ZnO, CuO and Se nanoparticles using marine alga *Sargassum swartzii* (*S. swartzii*); secondly, to isolate and molecular characterization of *V. parahaemolyticus* using 16S rRNA gene sequence and PCR analysis; further, to study anti-bacterial activity against newly isolated bacterial pathogen *V. parahaemolyticus* using biogenic prepared ZnO, CuO and Se nanoparticles; and finally, interaction of nanomaterials (ZnO, CuO and Se) with *V. parahaemolyticus* has been carried out using SEM-EDAX studies.

Materials and methods

Seaweed collection and preparation of extract

Brown macro alga *S. swartzii* was collected from Mandapam, Rameswaram (9.28° N 79.12° E), India (Fig. S1). The collected macro alga was washed with distilled water to remove the debris and other contaminants. The seaweed sample was then dried in shade and powdered using an electronic blender. About 10 g of powdered seaweed sample was dissolved in 1 L of distilled water and incubated in a shaker (1000 rpm) overnight under room temperature. Finally, the

extracts were filtered using Whatman filter paper no.1 and the filtrate was used for the preparation of nanomaterials.

Preparation of ZnO nanoparticles

Seaweed-stabilized ZnO nanoparticles were synthesized using co-precipitation method [30]. Briefly, macro algal extract (80 mL) was added with 400 mL of 0.1 M concentration of Zinc acetate [$\text{Zn}(\text{CH}_3\text{COO})_2 \cdot 2\text{H}_2\text{O}$, Merck with 99.0% purity] and mixed well using a magnetic stirrer at 70 °C for 20 min. About 400 mL of 0.2 M NaOH aqueous solution (400 mL) was added drop wise into the reaction solution under continuous stirring condition for 3 h. After 3 h, white precipitates were obtained thus confirming the formation of $\text{Zn}(\text{OH})_2$. The precipitates were collected, dried and allowed for calcination at 400 °C for 4 h to obtain the purest form of ZnO nanoparticles.

Preparation of CuO nanoparticles

CuO nanoparticles were prepared at room temperature through co-precipitation technique [41] with some modifications. Briefly, in this experiment, 0.1 M aqueous solution of copper acetate [$\text{Cu}(\text{CH}_3\text{COO})_2 \cdot \text{H}_2\text{O}$, Merck with 98.0% purity] along with 40 mL of algal extract was kept under constant stirring for 30 min. Then, 0.2 M of NaOH aqueous solution was added drop-wise into the reaction mixture and allowed to proceed for 4 h after complete addition of NaOH. Further, the reaction solutions were incubated overnight at room temperature for settlement of nanoparticles as precipitates. The precipitates were separated using centrifugation at $5000 \times g$ for 10 min, washed several times with deionized water and dried at 80 °C for 12 h. The dried powder was calcinated at 400 °C for 4 h to obtain the CuO nanoparticles.

Preparation of Se nanoparticles

For the preparation of Se nanoparticles, selenous acid (H_2SeO_3 , Sigma-Aldrich with 98% purity) (3 mM) was mixed with 100 mL of algal extract under magnetic stirring condition. Then, 150 mL of freshly prepared ascorbic acid (1.056 g) solution was slowly added into the reaction mixture until brick red precipitates were formed. Further, the solution was centrifuged at $5000 \times g$ for 20 min and the pellet was washed with deionized water and dried to obtain Se nanoparticles.

Characterization

UV–Vis diffuse reflectance spectroscopy (DRS–UV) absorption spectra were obtained using a JASCO V670, Japan UV–Vis spectrometer in the range of 200–1000 nm. XRD analysis were performed using an RIGAKU miniflex 600

instrument equipped with Cu-K α radiation source in the 2θ range of 10–80°. Scanning electron microscopy (SEM, Hitachi S-4800) and the elemental composition was carried out using energy dispersive X-ray analysis (EDAX, Oxford Instruments). Transmission electron microscopy (TEM) was performed with an FEI Technai instrument working at 120 kV. The sample for TEM was prepared by dropping the dispersion on a carbon-coated copper grid and drying under ambient conditions.

Sample collection

White-leg shrimp *P. vannamei* that was empty gut, anorexia, lethargy and pale hepatopancreas with discoloration [42] collected from a shrimp farm in Ponneri, Chennai, India (13.3339° N, 80.1943° E) show clinical signs of AHPND such as severity of infection. The diseased shrimp samples were collected on ice and transferred immediately to the laboratory within 3 h of collection for microbiological analysis.

Bacterial isolation and identification

Hepatopancreas of collected shrimp was excised aseptically and inoculated into tryptic soy agar plates supplemented with 1.5% NaCl for 12 h. Further, enriched media were used for spread plating on thiosulfate-citrate-bile salts-sucrose (TCBS) agar plates and incubated at 30 °C for 16 h [43]. The individual colonies obtained from the mixed bacterial isolates were re-streaked to obtain pure isolates and then identified based on their physiological, morphological and biochemical characters before storage as glycerol stocks at –80 °C [44].

Molecular identification of *V. parahaemolyticus*

The isolates were cultured in tryptic soy broth (TSB) media overnight and the genomic DNA was extracted by phenol chloroform extraction technique. The genomic DNA was quantified using a Bio-spectrometer (Eppendorf kinetic, Germany) and stored at –80 °C for further analysis. 16S ribosomal RNA partial sequence was performed and the sequence homology of extracted 16S rRNA gene sequence was analyzed by NCBI BLAST. The similarity matrix of 16S rRNA gene sequence of strain was obtained using Phylogeny Interface Package (PHYLIP 3.9) [45] and the sequences were aligned using the CLUSTAL X program [46]. The phylogenetic tree was constructed based on Neighbour-Joining (NJ) method using the Kimura 2-Parameter Model by the MEGA 7 software package [47] and tested by bootstrap analysis based on 1000 resamplings (NJ). The evolutionary distances were computed using the Maximum Composite Likelihood method [48]. Newly identified bacterial sequence was submitted to the NCBI to obtain accession



number. Moreover, the isolates were further analyzed for the presence of the molecular markers genes (*toxR* and *tlh*) of *V. parahaemolyticus*. PCR was performed for virulence genes with respective primers such as *toxR* and *tlh* as per the protocol followed by Ananda Raja et al. [43] (Table S1).

Anti-bacterial activity using in vitro test

Well diffusion assay was performed on Mueller Hinton agar plates with 2% sodium chloride spread with 100 μL *V. parahaemolyticus* bacterial suspension (1×10^6 cells/mL). Under aseptic conditions, well (5 mm) was made and filled 10 μL with different concentration (10, 25, 50, 75 and 100 $\mu\text{g mL}^{-1}$) of ultra-sonicated biogenic nanomaterials (ZnO, CuO and Se) and control was maintained in the absence of nanoparticles. The plates were incubated for 24 h at 28 °C, the inhibition zone was measured with zone of reader. The assay was performed with four replication.

Moreover, the effect of nanoparticles (ZnO, CuO and Se) on the growth rate of *V. parahaemolyticus* grown in Mueller Hinton broth at the concentration of 1×10^6 cells/mL was studied. The bacterial suspension was treated with different concentration (50, 100, 150 and 200 $\mu\text{g mL}^{-1}$) of ZnO, CuO and Se nanoparticles and incubated at 28 °C \pm 1 °C. Growth rates were determined by measuring the optical density (OD) of *V. parahaemolyticus* suspension treated with ZnO, CuO and Se nanoparticles at 600 nm using UV–Vis spectrophotometer and each measurement was made at an interval of 3 h, respectively [23].

SEM and EDAX studies of *V. parahaemolyticus*-treated nanomaterials

The interaction and morphological changes in *V. parahaemolyticus* cells on treatment with and without ZnO, CuO and Se nanoparticles were carried out by SEM with EDAX studies according to the protocol of Arakha et al. [49] with some modifications. Briefly, 1 mL of bacterial culture (10^6 CFU mL^{-1}) were treated with 1 mg mL^{-1} of ZnO, CuO and Se nanoparticles for 5 h at 37 °C and centrifuged at $5000 \times g$ for 5 min at 4 °C. The pellets were collected, washed, and re-suspended in 1 X PBS buffer. One drop of the re-suspended untreated and treated cultures were put on glass cover slip and bacterial cells (untreated and treated) were fixed using 2.5% glutaraldehyde in 1 X PBS solution. Further, the slides were suspended with 1% tannic acid for 5 min and washed with double distilled water, followed by dehydration process using increasing concentration of ethanol series (30%, 50%, 70%, 90% and 100%) for each 10 min. The dehydrated cells were dried overnight and sputter coated with gold, the coated samples (untreated and treated) were observed under SEM (Hitachi S-4800). The elemental composition and elemental mappings were

carried out using energy dispersive X-ray analysis (Oxford Instruments).

Statistical analysis

In the present, statistical studies were carried out with graphpad prism 7.0 software package. The experimental results are expressed as mean \pm SD. A significant difference among the means of samples were obtained by Tukey's test and analysis of variance was performed by one-way ANOVA.

Results and discussion

DRS-UV analysis

Figure S2a, b, c depicts the room temperature DRS-UV spectrum of seaweed-stabilized ZnO, CuO and Se nanoparticles. The seaweed-stabilized ZnO nanoparticles exhibit strong absorption edge at around 395 nm that could be related to the wurtzite crystal structure of ZnO [50]. The observed absorption onset peak value (395 nm) is greater than the bulk ZnO (368 nm) [51]. This red shift in wavelength is mainly related to the structural morphologies, particles size and microstructures of the prepared samples [52, 53]. DRS-UV spectrum of seaweed-stabilized CuO nanoparticles (Fig. 2b), a typical excitation absorption peak were observed at around 260 nm which is in good agreement with the expected value of CuO nanoparticles [12]. This surface plasmon resonance (SPR) peaks confirms the presence of CuO nanoparticles [10]. From Fig. 2c, the absorption bands at around 233 and 258 nm which are located between 200 and 300 nm were mainly due to formation of Se nanoparticles. These results are in conformation with the previous reports [54, 55].

XRD analysis

Figure 1a, b, c shows the XRD pattern of seaweed-stabilized ZnO, CuO and Se nanoparticles. From Fig. 1a, all diffraction peaks are assigned to crystalline nature of ZnO with the hexagonal wurtzite structure. The data confirms with the standard JCPDS card No. 036–1451 [9]. The peaks were detected at 2θ values are 31.76°, 34.52°, 36.33°, 47.69°, 56.64°, 62.86°, 66.34°, 67.99°, 69.28°, 72.74° and 76.95° corresponds to the lattice (*hkl*) planes (100), (002), (101), (102), (110), (103), (200), (112), (201), (004) and (202) respectively. The typical XRD pattern of seaweed-stabilized CuO nanoparticles (Fig. 1b) confirms that the sample is highly crystalline in nature with monoclinic structure of CuO with JCPDS File No: 080–1916 [56]. There is no existence of other impurity peaks which confirms the phase pure formation of CuO nanoparticles. The diffraction

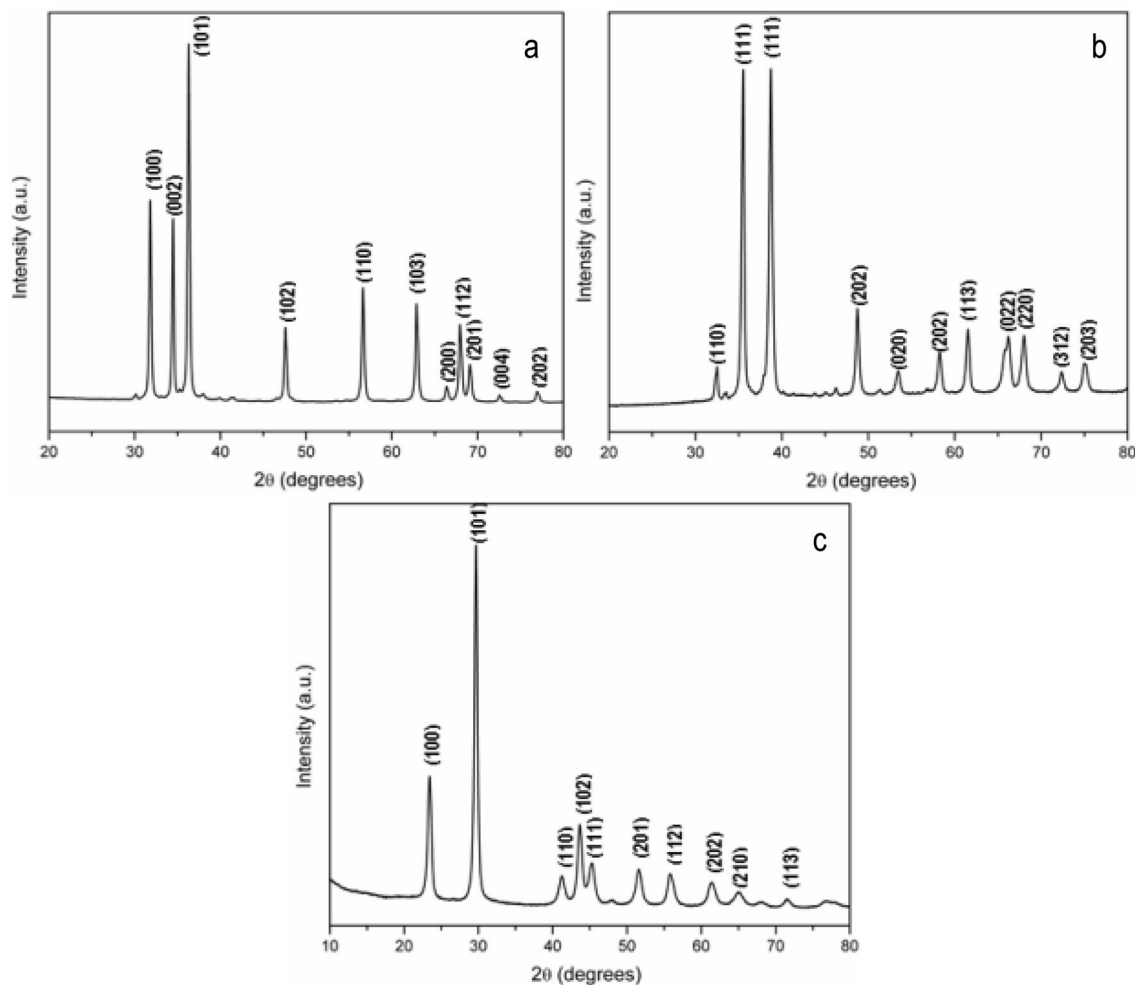


Fig. 1 XRD pattern of **a** ZnO nanoparticles; **b** CuO nanoparticles; **c** Se nanoparticles

peaks at $2\theta = 32.53^\circ, 35.55^\circ, 38.69^\circ, 48.72^\circ, 53.35^\circ, 58.33^\circ, 61.49^\circ, 66.15^\circ, 68.07^\circ, 72.28^\circ$ and 75.07° were assigned to (100), ($\bar{1}11$), (111), ($\bar{1}02$), (020), (202), ($\bar{1}13$), (022), (220), ($\bar{3}12$) and (203) planes, respectively. XRD pattern of seaweed-stabilized Se nanoparticles (Fig. 1c) confirms that all the diffraction peaks are consistent with the trigonal structure of Se nanoparticles. These results are in good agreement with the JCPDS File No: 006-0362) [57]. From the pattern, the diffraction peaks observed at 2θ values are $23.49^\circ, 29.75^\circ, 41.27^\circ, 43.63^\circ, 45.26^\circ, 47.83^\circ, 51.67^\circ, 55.70^\circ, 61.43^\circ, 65.12^\circ, 71.68^\circ$ and 76.97° corresponds to the following lattice (hkl) planes (100), (101), (110), (102), (111), (200), (201), (112), (202), (210), (113) and (301), respectively. From the XRD studies, the average particle size of seaweed-stabilized ZnO, CuO and Se nanoparticles were around 32.22, 32.15 and 21.12 nm, respectively which was calculated from the full width at half-maximum of the most intense peak of the XRD pattern using the Debye–Scherrer’s formula [58].

HR-SEM, EDAX and TEM analyses

Figure 2a, b depicts the SEM micrograph of ZnO nanoparticles which shows spherical morphology with smooth surface due to the stabilization of seaweed. Figure 2c shows the EDAX pattern of seaweed-stabilized ZnO nanoparticles, which confirms the presence of Zn and O. SEM images and EDAX pattern of seaweed-stabilized CuO nanoparticles is shown in Fig. 3a, b and Fig. 3c. It shows that the prepared nanoparticles exhibit well-defined smooth spherical surfaces which are rich in Cu and O. The surface morphology and elemental composition of the prepared Se nanoparticles were studied using SEM micrograph with EDAX pattern and are shown in Fig. 4a, b, c. Elemental composition of ZnO, CuO and Se nanoparticle weight ratio (wt%) was shown in Table S2a, b, c. TEM images of seaweed-stabilized ZnO, CuO and Se nanoparticles are shown in Fig. 5a, b, c. These result shows that the entire prepared samples exhibit well-defined spherical morphology with average particle size of



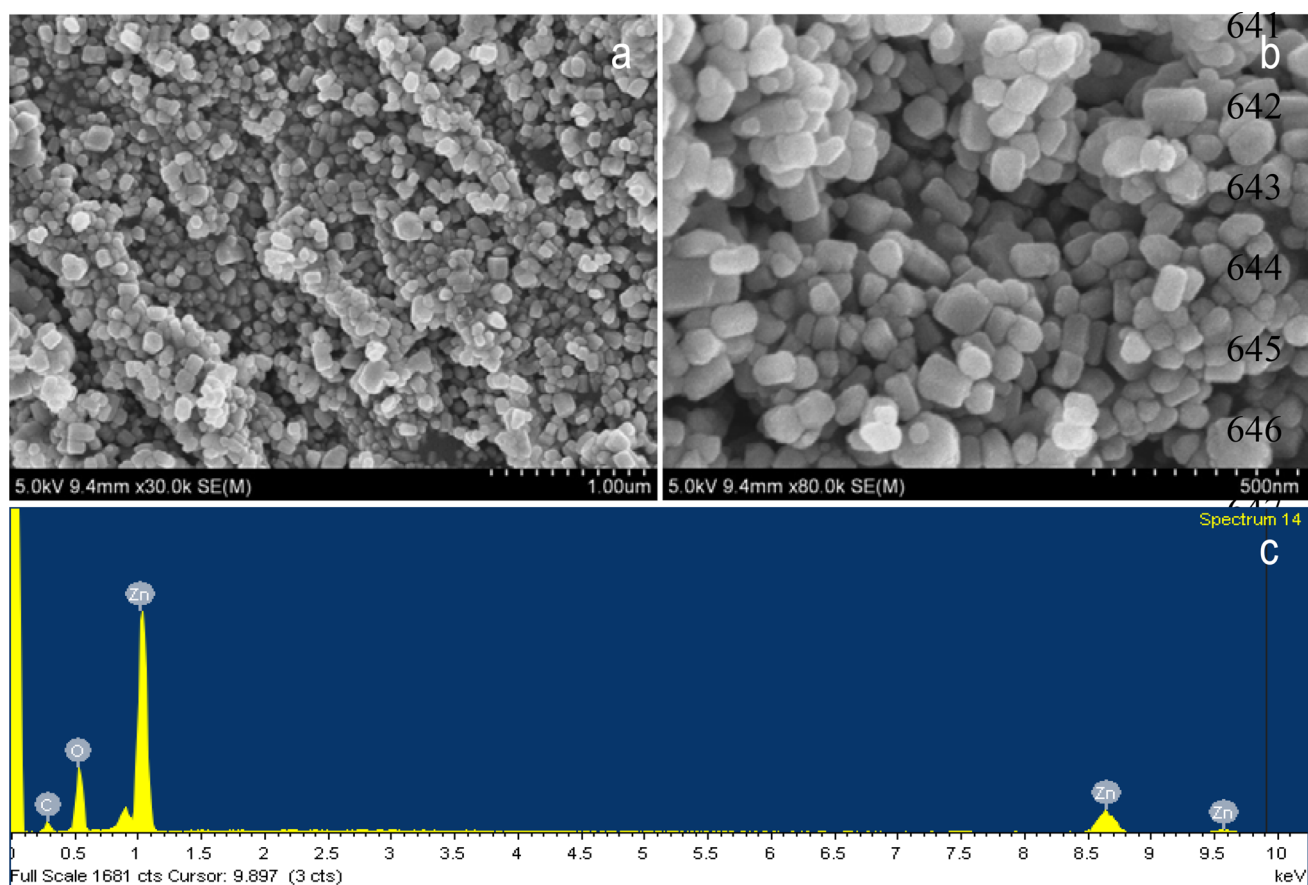


Fig. 2 a, b SEM images; c EDAX spectrum of ZnO nanoparticles

32 nm (ZnO), 32 nm (CuO) and 21 nm (Se) which is in good agreement with the well-defined XRD pattern. Figure 5d, e, f shows the histogram representing the size distribution of the ZnO, CuO and Se nanoparticles were obtained by digital analysis of images containing at least 100 nanoparticles.

Physiological, morphological and molecular identification

Based on the morphological characterization, the isolates were confirmed as *Vibrio* spp. The presence of green-colored circular colonies in rod shape confirmed it as *Vibrio* spp. Further, the results of 16S ribosomal RNA partial sequencing revealed that isolated strains of *Vibrio* sp, with closely related to *V. parahaemolyticus*. The forward/reverse showed that they were 98% homologous with *V. parahaemolyticus* RIMD 2210633 chromosome based on phylogenetic tree constructed and the NCBI accession number obtained as GRCORNICRA001 (Fig. 6). Further, molecular identification of *V. parahaemolyticus* based on specific virulent genes such as *toxR* and *tlh* was examined. The study shows that isolates were found to be positive for *Vp*-specific virulent strains *toxR* and *tlh* (Fig. 7). The *toxR*, transcriptional

activator is constantly found in AHPND causing *V. parahaemolyticus* isolates along with enterotoxin, and transmembrane regulatory protein *toxS*. Moreover, the strains are positive towards *toxR* and *tlh* gene in the present study, but they were negative to AP1, AP2, AP3 (*pirAvp*), and AP4 (*pirAvp* and *pirBvp*) genes which are responsible for causing AHPND in shrimp [59]. The results were in good agreement with the previous study carried out in the same sample collection region [43].

Anti-bacterial studies

Anti-bacterial test was performed by well diffusion assay which showed differences in the growth inhibition zone diameter (mm) between the three nanomaterials (ZnO, CuO and Se) against *V. parahaemolyticus* and their interaction were analyzed with a one-way ANOVA ($p=0.001$) (Table 1). The results indicated that all these nanoparticles caused growth inhibition of *V. parahaemolyticus*. The minimum inhibitory concentration (MIC) of ZnO, CuO and Se nanoparticles was found to be 25, 25 and 10 $\mu\text{g mL}^{-1}$ respectively. The dynamics of bacterial growth (*V. parahaemolyticus*) were also studied using 1×10^6 CFU/mL treated with

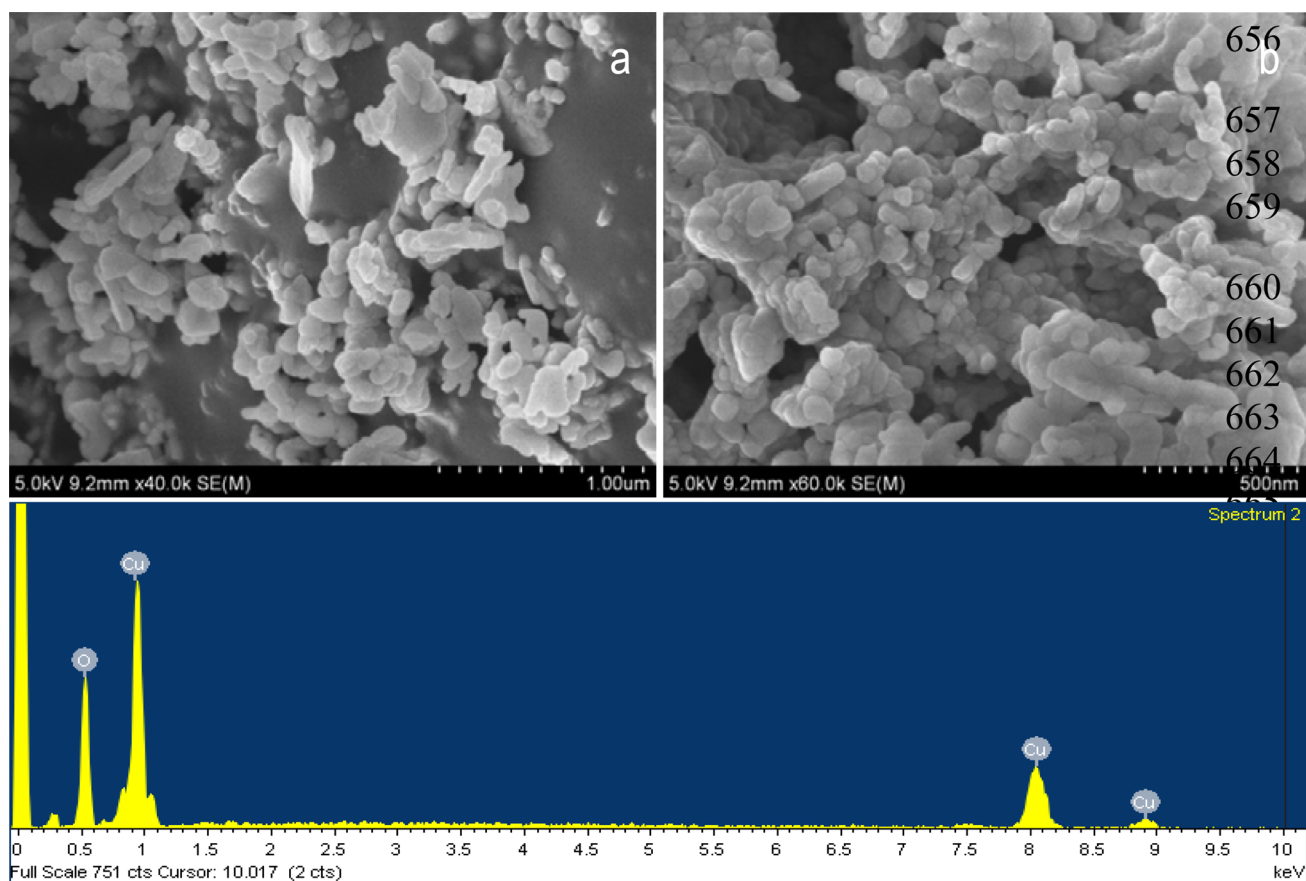


Fig. 3 a, b SEM images; c EDAX spectrum of CuO nanoparticle

different concentration (50, 100, 150 and 200 $\mu\text{g mL}^{-1}$) of ZnO, CuO and Se nanoparticles, respectively. The results showed increase in growth inhibition were observed during increased exposure time and dose (Fig.S3a-c). Various metal and metal oxide nanoparticles and their anti-bacterial activity have been documented well against diseases in aquatic organisms [45, 46, 60–64] among which few of the studies were reported with anti-bacterial activity of silver nanoparticles against AHPND causing *V. parahaemolyticus* [65–69]. A study reported AgNP impregnated with bacterial cellulose (BC) exhibited high vibriocidal activity against *V. parahaemolyticus* with zone of inhibition (21 ± 3.1 mm) at the concentration of 10 $\mu\text{g/mL}$. The possible mechanism of inhibition might be associated with binding of AgNP to bacterial cell membrane and interactions with the thiol groups of bacterial protein [67].

Interaction studies of nanomaterials (ZnO, CuO and Se) and *V. parahaemolyticus* cells by SEM and EDAX

The interaction studies and morphological changes in the untreated and ZnO/CuO/Se nanoparticles-treated *V.*

parahaemolyticus cells were observed by SEM. Figure 8 shows normal *V. parahaemolyticus* cells were found to be typically rod-shaped and almost same size with no visible damage on the cell surface. However, the morphology of ZnO, CuO and Se nanoparticles-treated *V. parahaemolyticus* cells changed significantly. The images (Figs. 9a, b, 10a, b and 11a, b) clearly show more clumping, topological changes in bacterial membrane and membrane rupture in the ZnO, CuO and Se nanoparticles-treated cells than the untreated cells. Further, major damages were observed by the formation of ‘pits’ in their cell envelope and clusters of nanoparticles (ZnO, CuO and Se) were found and anchored to the *V. parahaemolyticus* cells surface. As results of Figs. 9a, b, 10a, b and 11a, b show the bacterial membranes were abnormal textures such as membrane rupture and membrane blebs. The elemental compositions, mappings and distribution (Zn, O and C), (Cu, O and C) and (Se, O and C) of ZnO, CuO and Se nanoparticles were observed in the treated *V. parahaemolyticus* cells Figs. 9c, d, 10c, d and 11c, d. The quantitative data of elemental composition were shown in inset Figs. 9d, 10d and 11d. Various studies have been conducted to reveal the anti-microbial activities of nanoparticles against gram-negative and gram-positive bacteria, however

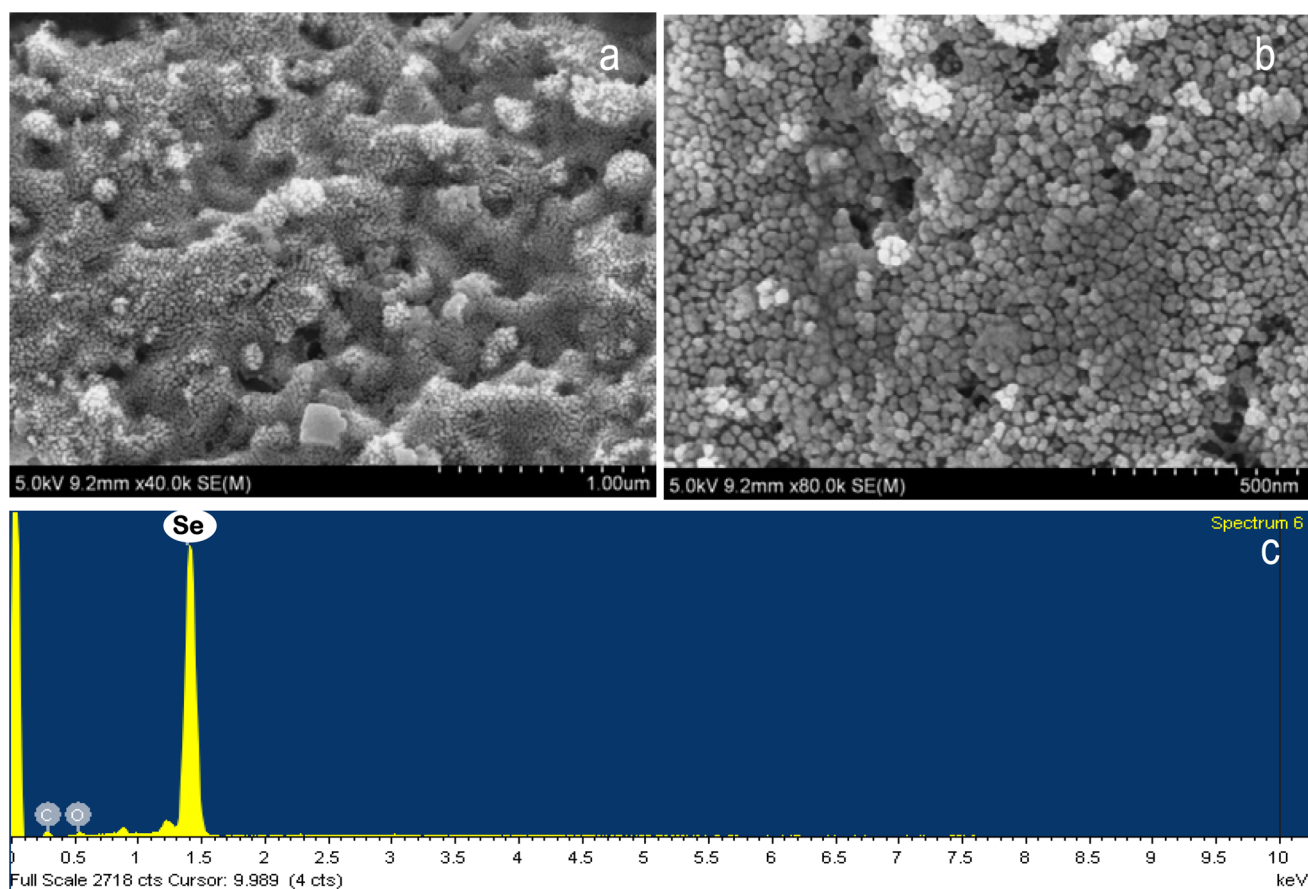


Fig. 4 a, b SEM images; c EDAX spectrum of Se nanoparticles

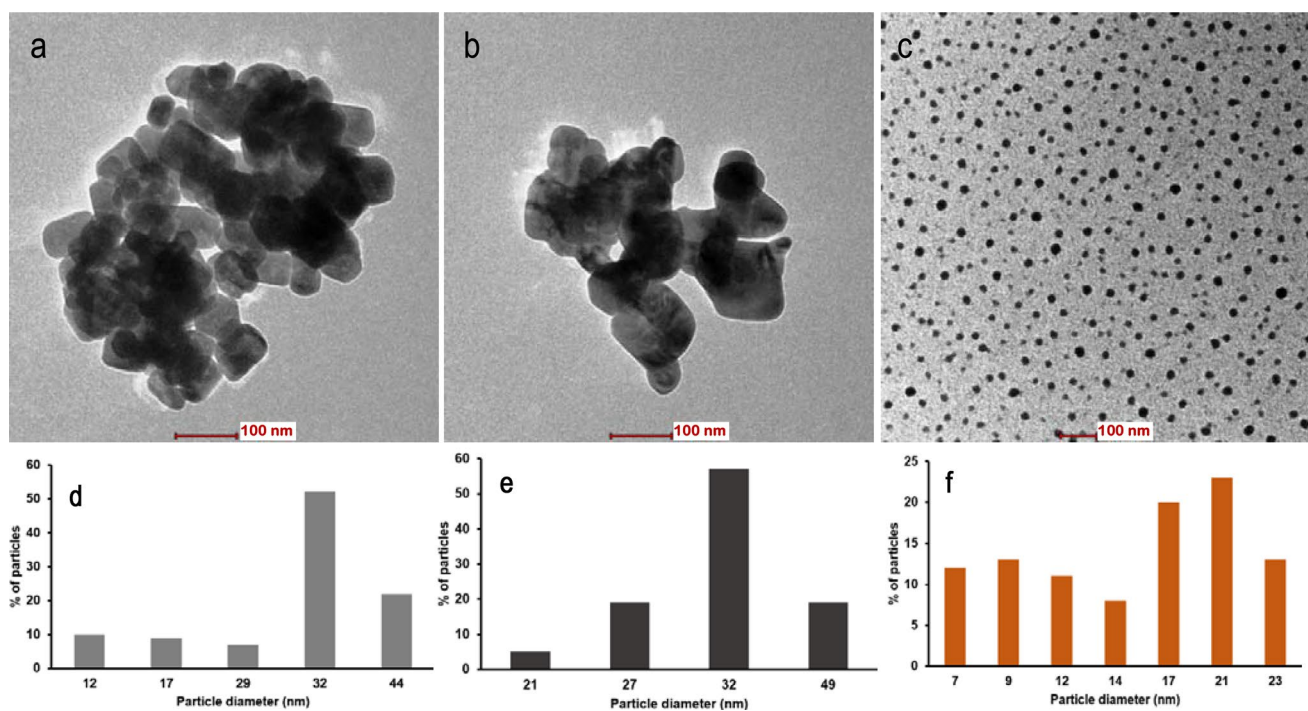


Fig. 5 TEM images of a ZnO nanoparticles; b CuO nanoparticles; c Se nanoparticles; d, e, f nanoparticles size distribution



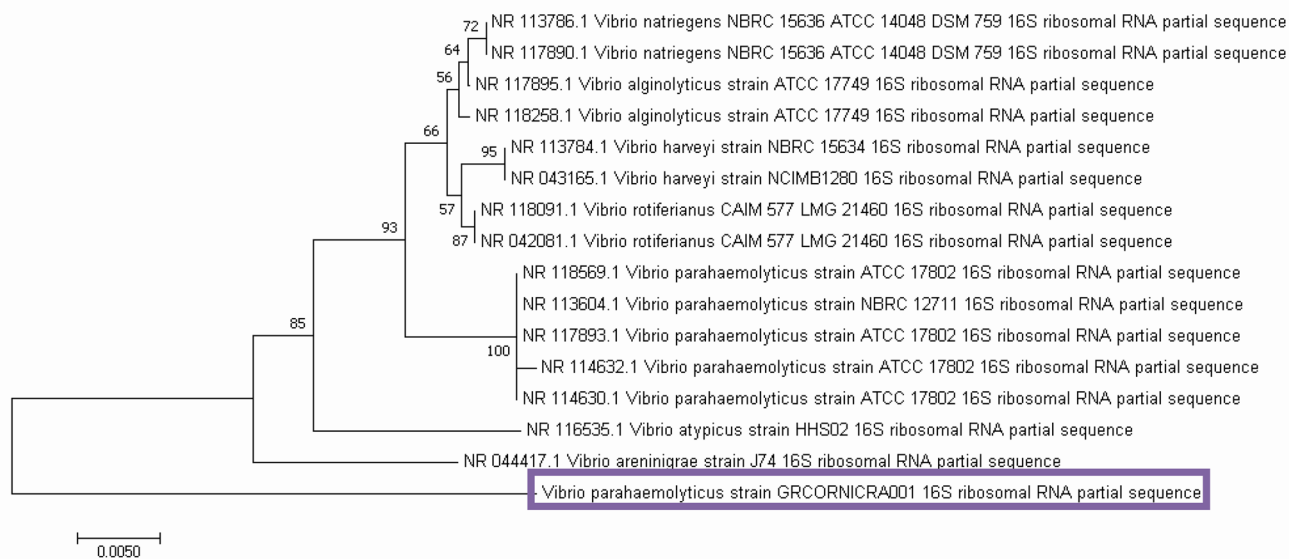


Fig. 6 Phylogenetic tree of the strain *V. parahaemolyticus* GRCORNICRA001 based on 16S rRNA gene sequence

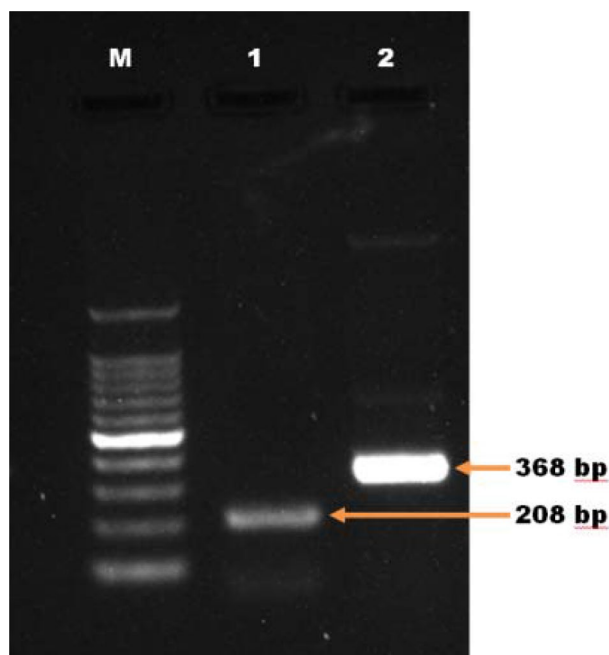


Fig. 7 Agarose gel showing the PCR product specific to 1. *VP-tlh* (thermolabile haemolysin) gene; 2. *VP-toxR* gene; M–100 bp marker

there is a lack of mechanistic insights underlying the concept to be explored. To date, limited research work is available on the antimicrobial activity of metal nanomaterials on *V. parahaemolyticus*. Comprehensive image shows (Fig. 12) the structural changes and anti-bacterial mechanism of bacterial pathogen (*V. parahaemolyticus*) treated with different nanomaterials (ZnO, CuO and Se).

Generally, the anti-microbial mechanism of ZnO nanoparticles on other bacterial strains includes release of Zn^{2+} ions, cell wall damage and generation of ROS, lipid peroxidation, protein and DNA damage. Increase in ROS generation leads to membrane leakage of proteins, nucleic acids and release of Zn^{2+} ions disrupts the cell membrane and intracellular components [70, 71]. The recent study on the antimicrobial effect of ZnO nanoparticles on gram negative bacteria shows that efficiency of antimicrobial activity is mainly depends on the interfacial potential, which is the interaction of nanoparticles surface with the bacterial membrane. Further, it shows that ZnO nanoparticles with positive surface potential upon interaction with bacteria having negative surface potential have significant anti-microbial activity [69]. Based on this study, it

Table 1 In vitro antimicrobial activity of biogenic nanomaterials (ZnO, CuO and Se) against AHPND causing *Vibrio parahaemolyticus* by well diffusion assay ($n=3$)

Nanomaterials	Zone of inhibition (mm)				
	10 ($\mu\text{g mL}^{-1}$)	25 ($\mu\text{g mL}^{-1}$)	50 ($\mu\text{g mL}^{-1}$)	75 ($\mu\text{g mL}^{-1}$)	100 ($\mu\text{g mL}^{-1}$)
Zinc oxide (ZnO)	3 ± 1.25	5 ± 1.35	7 ± 2.2	11 ± 1.0	15 ± 2.0
Copper oxide (CuO)	4 ± 0.35	7 ± 2.0	9 ± 1.35	11 ± 1.25	13 ± 1.20
Selenium (Se)	5 ± 0.50	7 ± 1.36	10 ± 2.2	11 ± 1.0	13 ± 1.65



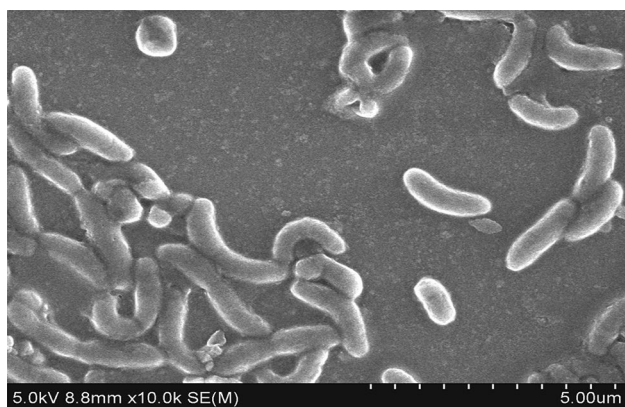


Fig. 8 SEM visualization of *V. parahaemolyticus* normal cells

is concluded that interfacial potential causing attachment of nanoparticle to bacterial cells followed by neutralization of bacterial surface potential leads to production of ROS inside the cells resulting in the cell death. In addition, our experiment with CuO nanoparticles-exposed *V. parahaemolyticus* showed the formation of blebs on the surface which is the signature of vibrio species. The results of the study are in good agreement with previous study on CuO nanoparticles-treated *V. anguillarum*. The blebs formed are the result of starvation during growth arrest and also exposure to the toxicant in the absence of nutrients [72]. The mechanism of antimicrobial activity of CuO nanoparticles is based on the electrostatic attraction between Cu^{2+} and plasma membrane which causes membrane damage leading to killing of cells [73]. This study

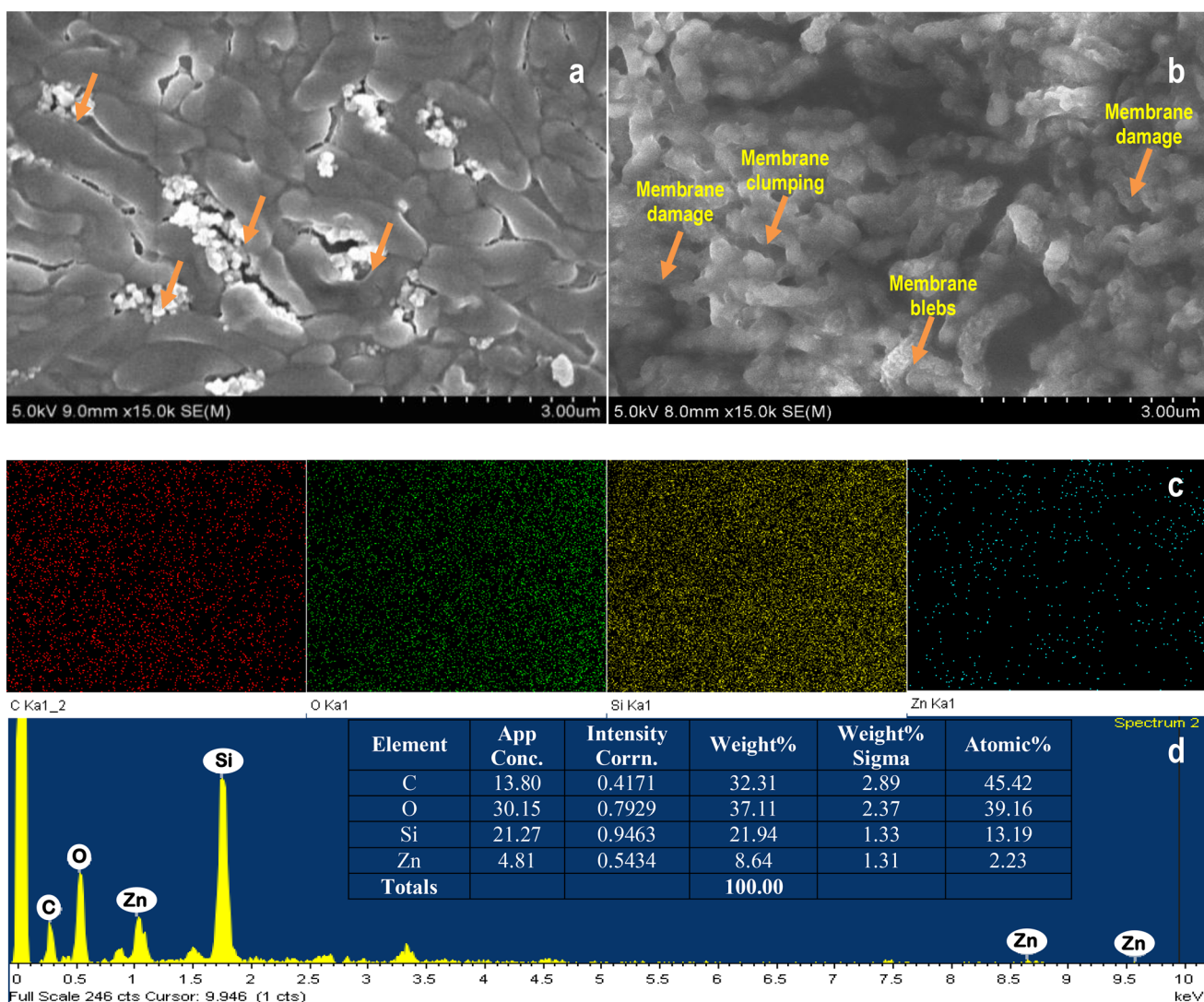


Fig. 9 SEM visualization of **a** ZnO nanoparticles-treated *V. parahaemolyticus*; **b** showing membrane clumping, membrane blebings and membrane damage in ZnO nanoparticles-treated cells; **c** element-

tal mapping of ZnO nanoparticles-treated *V. parahaemolyticus*; **d** EDAX spectrum of ZnO nanoparticles-treated *V. parahaemolyticus*

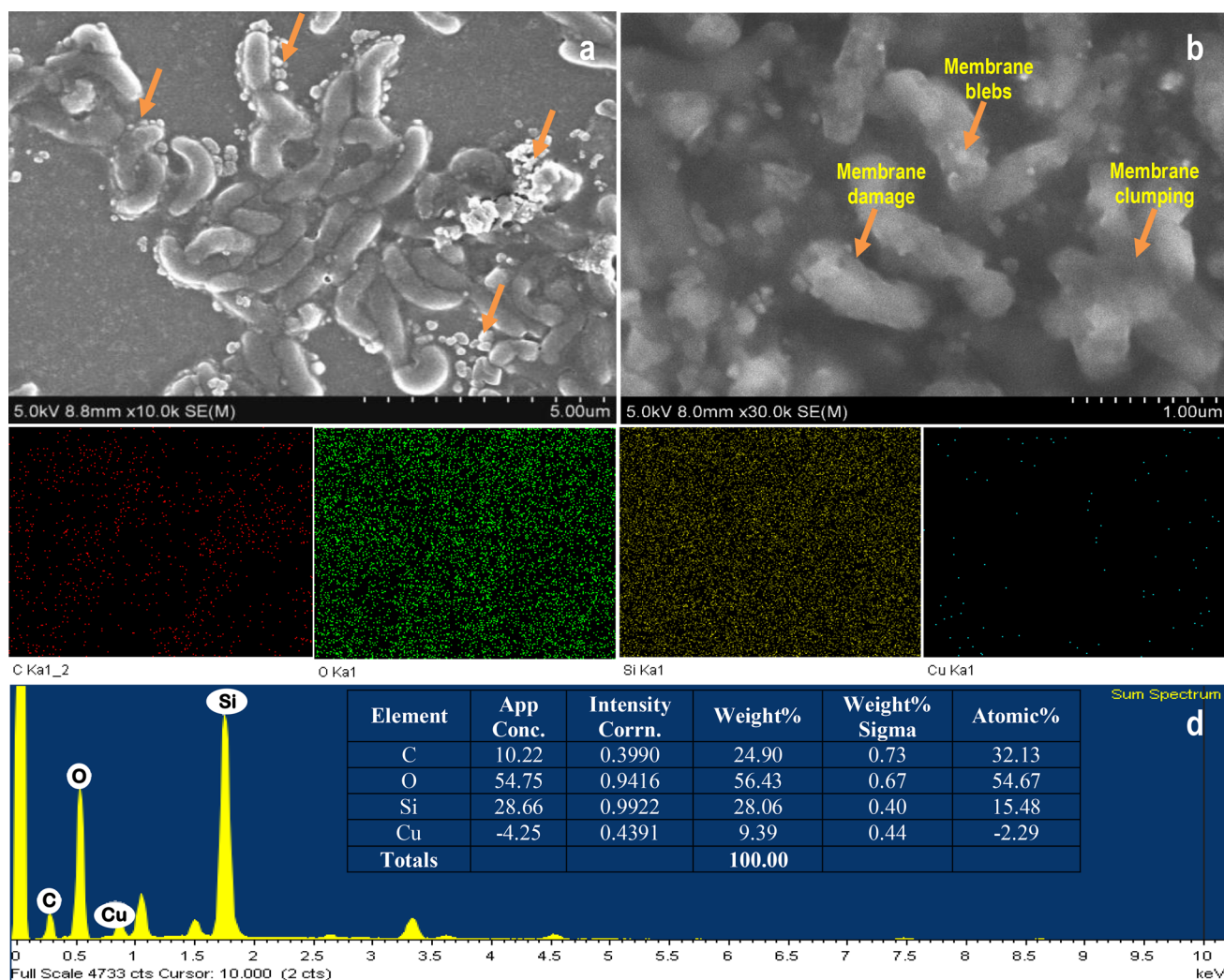


Fig. 10 SEM visualization of **a** CuO nanoparticles-treated *V. parahaemolyticus*; **b** showing membrane blebbs and membrane damage in CuO nanoparticles-treated cells; **c** elemental mapping of CuO

nanoparticles-treated *V. parahaemolyticus*; **d** EDAX spectrum of CuO nanoparticles-treated *V. parahaemolyticus*

on Se nanoparticles showed that the damage of cell surface and its changes in morphology. This is in good agreement with the previous study on anti-bacterial activity of Se nanoparticles as a nanohybrid system [74]. The presence of negatively charged lipopolysaccharide on the surface of bacteria expected to be the reason for high repulsiveness between bacteria and Se nanoparticles. Hence, bacteria with lower surface charge enhance the interaction with the nanoparticles and results in the deposition of nanoparticles on the surface leading to the adverse effects on bacterial cells. Overall, it is concluded that surface characteristics and cell wall composition of bacterium and surface net charge of nanoparticles is a critical factor for an enhanced anti-microbial activity. However, future studies on the anti-bacterial influence of these nanoparticles on other shrimp pathogens, in vivo studies on shrimp and

their plausible mechanism are necessary to evaluate its potential use as a bactericidal material in aquaculture.

Conclusions

ZnO, CuO and Se nanoparticles were successfully synthesized using *S. swartzii* and their physico-chemical characteristics were carried out using various spectroscopic and microscopic techniques. The ZnO, CuO and Se nanoparticles have absorption at 395 nm, 260 nm and 233–258 nm in DRS-UV spectrum. X-ray diffraction spectrum confirms 2θ values corresponding to the presence of ZnO, CuO and Se with JCPDS. SEM micrographs of ZnO, CuO and Se nanoparticles which shows spherical morphology. TEM images shows well-defined spherical morphology



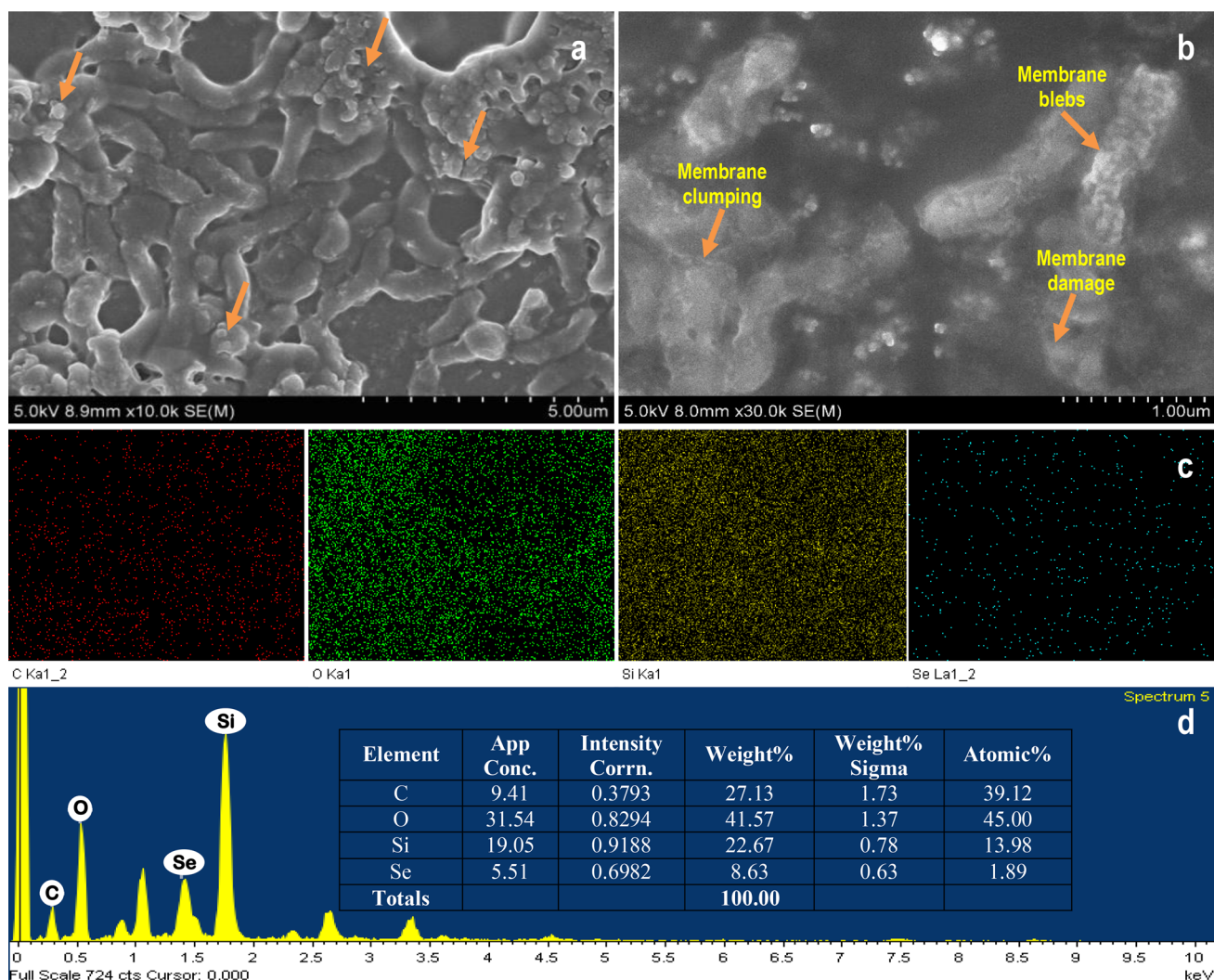


Fig. 11 SEM visualization of **a** Se nanoparticles-treated *V. parahaemolyticus*; **b** showing membrane blebbings and membrane damage in Se nanoparticles-treated cells; **c** elemental mapping of Se

nanoparticles-treated *V. parahaemolyticus*; **d** EDAX spectrum of Se nanoparticles-treated *V. parahaemolyticus*

with average particle size of 32 nm (ZnO), 32 nm (CuO) and 21 nm (Se). The new bacterial strains were isolated from infected shrimp sample and identified as *V. parahaemolyticus* based on 16S ribosomal RNA sequencing and presence of specific virulent genes (*toxR* and *tlh*). The biogenic nanomaterials (ZnO, CuO and Se) exhibited potent anti-bacterial efficiency against *V. parahaemolyticus*. The interaction of nanomaterials (ZnO, CuO and Se)

with *V. parahaemolyticus* was analyzed using SEM which revealed that the attachment of nanoparticles on the surface of cell membrane causes non viability of cells. The present study confirms the enhanced anti-bacterial efficiency of seaweed-stabilized nanoparticles (ZnO, CuO and Se). Hence, the prepared nanoparticles can be formulated as a bactericidal material against the aquaculture pathogens in efficient disease control.

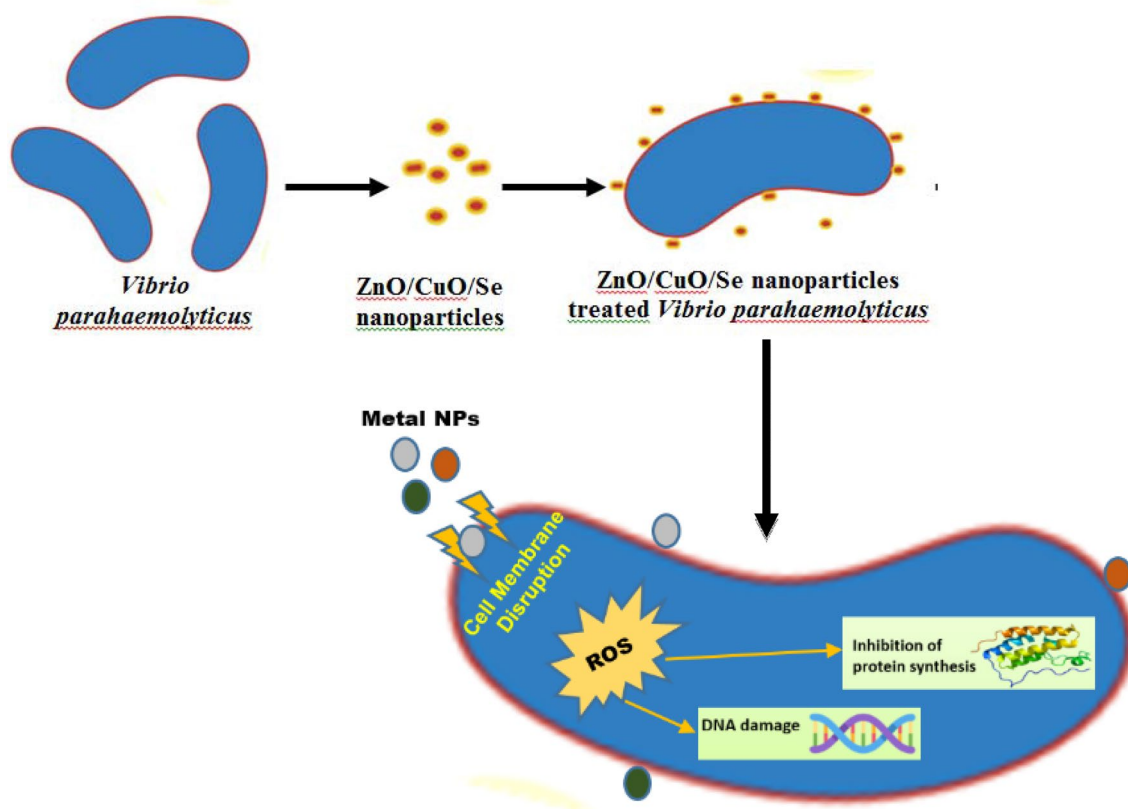


Fig. 12 Schematic diagram showing the nanomaterials interaction and their mechanism of anti-bacterial activity

Acknowledgement We thank the National Innovations on Climate Resilient Agriculture (NICRA), Indian Council of Agricultural Research (ICAR), and the Government of India for their financial support (F.No.2-13(8)/19-20 NICRA).

Compliance with ethical standards

Conflict of interest All authors sincerely declare that they have no known competing financial interests.

References

- Kumar, B.K., Deekshit, V.K., Raj, J.R.M., Rai, P., Shivanagowda, B.M., Karunasagar, I., Karunasagar, I.: Diversity of *Vibrio parahaemolyticus* associated with disease outbreak among cultured *Litopenaeus vannamei* (Pacific white shrimp) in India. *Aquaculture* **433**, 247–251 (2014)
- De Schryver, P., Defoirdt, T., Sorgeloos, P.: Early mortality syndrome outbreaks: a microbial management issue in shrimp farming? *PLOS Pathog.* **10**, e1003919 (2014)
- Lightner, D.V., Redman, R.M., Pantoja, C.R., Noble, B.L., Tran, L.H.: Early mortality syndrome affects shrimp in Asia. *Glob. Aquacult.* **15**, 40 (2012)
- FAO.: Report of the FAO/MARD technical workshop on early mortality syndrome (EMS) or acute hepatopancreatic necrosis syndrome (AHPND) of cultured shrimp (under TCP/VIE/3304), 2013. Hanoi, Viet Nam, 25–27 June 2013. FAO Fisheries and Aquaculture Report No. 1053. Rome, Italy, pp. 54 (2013)
- Heuer, O.E., Kruse, H., Grave, K., Collignon, P., Karunasagar, I., Angulo, F.J.: Human health consequences of use of antimicrobial agents in aquaculture. *Clin. Infect. Dis.* **49**, 1248–1253 (2009)
- Romero, J., Gloria, C., Navarrete, P.: Antibiotics in Aquaculture—Use, Abuse and Alternatives, in Health and Environment in Aquaculture. IntechOpen, London (2012)
- Rathna Kumari, P., Kolanchinathan, P., Siva, D., Abirami, B., Masilamani, V., John, G., Achiraman, S., Balasundaram, A.: Antibacterial efficacy of seagrass *Cymodocea serrulata* engineered silver nanoparticles against prawn pathogen *Vibrio parahaemolyticus* and its combative effect on the marine shrimp *Penaeus monodon*. *Aquaculture* **493**, 158–164 (2018)
- Kumar, R., Ng, T.H., Wang, H.C.: Acute hepatopancreatic necrosis disease in penaeid shrimp. *Rev. Aquacult.* **12**, 1867–1880 (2020)
- Ometto, F.B., Carbonio, E.A., Teixeira-Neto, E., Villullas, H.M.: Changes induced by transition metal oxides in Pt nanoparticles unveil the effects of electronic properties on oxygen reduction activity. *J. Mater. Chem. A* **7**, 2075–2086 (2019)
- George, J.M., Antony, A., Mathew, B.: Metal oxide nanoparticles in electrochemical sensing and biosensing: A review. *Microchim. Acta* **185**, 358 (2018)
- Akbari, A., Amini, M., Tarassoli, A., Eftekhari-Sis, B., Ghasemian, N., Jabbari, E.: Transition metal oxide nanoparticles as efficient catalysts in oxidation reactions. *Nano-Struct. Nano-Objects* **14**, 19–48 (2018)
- Zak, A.K., Majid, W.H., Abhrishami, M.E., Yousefi, R.: X-ray analysis of ZnO nanoparticles by Williamson-Hall and size-strain plot methods. *Solid State Sci.* **13**, 251–256 (2011)



13. Abo-zeid, Y., Williams, G.R.: The potential anti-infective applications of metal oxide nanoparticles: A systematic review. *Wires Nanomed. Nanobiotechnol.* **12**, e1592 (2020)
14. Hosseini-Koupaei, M., Shareghi, B., Saboury, A.A., Davar, F., Sirotkin, V.A., Hosseini-Koupaei, M.H.: Catalytic activity, structure and stability of proteinase K in the presence of biosynthesized CuO nanoparticles. *Int. J. Biol. Macromol.* **122**, 732–744 (2019)
15. Anbuvaran, M., Ramesh, M., Viruthagiri, G., Shanmugam, N., Kannadasan, N.: *Anisochilus carnosus* leaf extract mediated synthesis of zinc oxide nanoparticles for antibacterial and photocatalytic activities. *Mater. Sci. Semicond. Process.* **39**, 621–628 (2015)
16. Sutradhar, P., Saha, M., Maiti, D.: Microwave synthesis of copper oxide nanoparticles using tea leaf and coffee powder extracts and its antibacterial activity. *J. Nanostruct. Chem.* **4**, 86 (2014)
17. Yusof, A.M., Yuson, S.: Synthesis and structural properties of nanoselenium-supported MCM-41 material. *Syn. React. Inorg. Met. Org. Nano-Met. Chem.* **46**, 747–753 (2015)
18. Gautam, P.K., Kumar, S., Tomar, M.S., Singh, R.K., Acharya, A., Kumar, S., Ram, B.: Selenium nanoparticles induce suppressed function of tumor associated macrophages and inhibit Dalton's lymphoma proliferation. *Biochem. Biophys. Rep.* **12**, 172–184 (2017)
19. Adil, S.F., Assal, M.E., Khan, M., Al-Warthan, A., Siddiqui, M.R.H., Liz-Marzán, L.M.: Biogenic synthesis of metallic nanoparticles and prospects toward green chemistry. *Dalton Trans.* **44**, 9709–9717 (2015)
20. Hulkoti, N.I., Taranath, T.C.: Biosynthesis of nanoparticles using microbes-A review. *Colloids and Surf. B: Biointerf.* **121**, 474–483 (2014)
21. Bresien, J., Hinz, A., Schulz, A., Villinger, A.: Trapping of transient, heavy pnicogen-centred biradicals. *Dalton Trans.* **47**, 4433–4436 (2018)
22. Govindaraju, K., Kiruthiga, V., Ganesh, K.V., Singaravelu, G.: Extracellular synthesis of silver nanoparticles by a marine alga, *Sargassum wightii* Greville and their antibacterial effects. *J. Nanosci. Nanotechnol.* **9**, 5497–5501 (2009)
23. Uma, K.S., Govindaraju, K., Ganesh, K.V., Stalin, D.T., Karthick, V., Singaravelu, G., Elanchezhian, M.: Size controlled biogenic silver nanoparticles as antibacterial agent against isolates from HIV infected patients. *Spectrochim. Acta Part A.* **144**, 266–272 (2015)
24. Govindaraju, K., Karthikeyan, K., Alsagaby, S., Singaravelu, G., Premanathan, M.: Green synthesis of silver nanoparticles for selective toxicity towards cancer cells. *IET Nanobiotechnol.* **9**, 325–330 (2015)
25. Uma Suganya, K.S., Govindaraju, K., Ganesh Kumar, V., Karthick, V., Krupakar, P.: Pectin mediated gold nanoparticles induces apoptosis in mammary adenocarcinoma cell lines. *Int. J. Biol. Macromol.* **93**, 1030–1040 (2016)
26. Venkatachalam, M., Govindaraju, K., Mohamed, S.A., Tamilselvan, S., Ganesh, K.V., Singaravelu, G.: Functionalization of gold nanoparticles as anti-diabetic nanomaterial. *Spectrochim. Acta Part A.* **116**, 331–336 (2013)
27. Khaleel Basha, S., Govindaraju, K., Manikandan, R., Ahn, J.S., Bae, E.Y., Singaravelu, G.: Phytochemical mediated gold nanoparticles and their PTP 1B inhibitory activity. *Colloids Surf. B* **75**, 405–409 (2010)
28. Vinodhini, A., Govindaraju, K., Singaravelu, G., Mohamed, S.A., Ganesh, K.V.: Cardioprotective potential of biobased gold nanoparticles. *Colloids Surf. B* **117**, 480–486 (2014)
29. Prerna, D.I., Govindaraju, K., Tamilselvan, S., Kannan, M., Raja, K., Subramanian, K.S.: Seaweed-based biogenic ZnO nanoparticles for improving agro-morphological characteristics of rice (*Oryza sativa* L.). *J. Plant Growth Regul.* **39**, 717–728 (2020)
30. Govindaraju, K., Tamilselvan, S., Kannan, M., Kathickeyan, D., Doron, S., Sumit, C.: Nano-micronutrients [γ -Fe₂O₃ (iron) and ZnO (zinc)]: green preparation, characterization, agro-morphological characteristics and crop productivity studies in two crops (rice and maize). *New J. Chem.* **44**, 11373–11383 (2020)
31. Singaravelu, G., Arockiyamari, J.S., Ganesh Kumar, V., Govindaraju, K.: A novel extracellular synthesis of monodisperse gold nanoparticles using marine algae, *Sargassum wightii*. *Colloids Surf. B* **57**, 97–101 (2007)
32. Wijesekara, I., Pangestuti, R., Kim, S.K.: Biological activities and potential health benefits of sulfated polysaccharides derived from marine algae. *Carbohydr. Polym.* **84**, 14–21 (2011)
33. Vasantharaja, R., Stanley Abraham, L., Jyotsna, J., Seedeivi, P., Sathishkannan, G., Thirugnanasambandam, R., Kirubakaran, R.: Sulfated polysaccharide from *Sargassum tenerrimum* attenuates oxidative stress induced reactive oxygen species production in *in vitro* and in zebrafish model. *Carbohydr. Polym.* **203**, 441–449 (2019)
34. Rather, M.A., Sharma, R., Aklakur, M., Ahmad, S., Kumar, N., Khan, M., Ramya, V.L.: Nanotechnology: A novel tool for aquaculture and fisheries development-A prospective mini-review. *Fisheries Aquacult. J.* **16**, 1–5 (2011)
35. Govindaraju, K., Prerna, D.I., Veeramani, V., Ashok, T.K., Tamilselvan, S.: Application of nanotechnology in diagnosis and disease management of white spot syndrome virus (WSSV) in aquaculture. *J. Clust. Sci.* **31**, 1163–1171 (2020)
36. Kulabhusan, P.K., Rajwade, J.M., Vimal, S., Taju, G., Sahul Hameed, A.S., Paknikar, K.M.: Field-usable lateral flow immunoassay for the rapid detection of white spot syndrome virus (WSSV). *PLoS ONE* **12**, e0169012 (2017)
37. Zhou, X., Wang, Y., Gu, Q., Li, W.: Effects of different dietary selenium sources (selenium nanoparticle and selenomethionine) on growth performance, muscle composition and glutathione peroxidase enzyme activity of crucian carp (*Carassius auratus gibelio*). *Aquaculture* **291**, 78–81 (2009)
38. Rather, M.A., Sharma, R., Gupta, S., Ferosekhan, S., Ramya, V.L., Jadhao, S.B.: Chitosan-nanoconjugated hormone nanoparticles for sustained surge of gonadotropins and enhanced reproductive output in female fish. *PLoS ONE* **8**, e57094 (2013)
39. Rajesh Kumar, S., Ishaq Ahmed, V.P., Parameswaran, V., Sudhakaran, R., Sarath Babu, V., Sahul Hameed, A.S.: Potential use of chitosan nanoparticles for oral delivery of DNA vaccine in Asian sea bass (*Lates calcarifer*) to protect from *Vibrio (Listonella) anguillarum*. *Fish Shellfish. Immunol.* **25**, 47–56 (2008)
40. National Research Council: Nutrient Requirements of Fish and Shrimp. The National Academies Press, Washington (2011)
41. Muthamil Selvan, S., Vijai Anand, K., Govindaraju, K., Tamilselvan, S., Ganesh Kumar, V., Subramanian, K.S., Kannan, M., Raja, K.: Green synthesis of copper oxide nanoparticles and mosquito larvicidal activity against dengue, zika and chikungunya causing vector *Aedes aegypti*. *IET Nanobiotechnol.* **12**, 1042–1046 (2018)
42. Soto-Rodriguez, S.A., Gomez-Gil, B., Lozano, R., del Rio-Rodriguez, R., Dieguez, A.L., Romalde, J.L.: Virulence of *Vibrio Harveyi* responsible for the “Bright-red” syndrome in the Pacific white shrimp *Litopenaeus vannamei*. *J. Invert. Pathol.* **109**, 307–317 (2012)
43. Ananda Raja, R., Sridhar, R., Balachandran, C., Palanisammi, A., Ramesh, S., Nagarajan, K.: Pathogenicity profile of *Vibrio parahaemolyticus* in farmed Pacific white shrimp *Penaeus vannamei*. *Fish Shellfish. Immunol.* **67**, 368–381 (2017)
44. Alsina, M., Blanch, A.R.: A set of keys for biochemical identification of environmental *Vibrio* species. *J. Appl. Bacteriol.* **76**, 79–85 (1994)
45. Felsenstein, J.: Confidence limit on phylogenies: an approach using the bootstrap. *Evolution* **39**, 783–791 (1985)




46. Thompson, J.D., Gibson, T.J., Plewniak, F., Jeanmougin, F., Higgins, D.G.: The CLUSTAL_X windows interface: flexible strategies for multiple sequence alignment aided by quality analysis tools. *Nucleic Acids Res.* **25**, 4876–4882 (1997)
47. Kumar, S., Stecher, G., Tamura, K.: MEGA7: molecular evolutionary genetics analysis version 7.0 for bigger datasets. *Mol. Biol. Evol.* **33**, 1870–1874 (2016)
48. Tamura, K., Nei, M., Kumar, S.: Prospects for inferring very large phylogenies by using the neighbor-joining method. *Proc. Nat. Acad. Sci. USA* **101**, 11030–11035 (2004)
49. Arakha, M., Saleem, M., Mallick, B.C., Jha, S.: The effects of interfacial potential on antimicrobial propensity of ZnO nanoparticle. *Sci. Rep.* **5**, 9578 (2015)
50. Wahab, R., Ansari, S., Kim, Y., Seo, H., Kim, G., Khang, G., Shin, H.S.: Low temperature solution synthesis and characterization of ZnO nano-flowers. *Mater. Res. Bull.* **42**, 1640–1648 (2007)
51. Zeng, X., Yang, J., Shi, L., Li, L., Gao, M.: Synthesis of multi-shelled ZnO hollow microspheres and their improved photocatalytic activity. *Nanoscale Res. Lett.* **9**, 468 (2014)
52. Prakash, T., Jayaprakash, R., Neri, G., Kumar, S.: Synthesis of ZnO nanostructures by microwave irradiation using albumen as a template. *J. Nanopart.* **2013**, 274894 (2013)
53. Zak, A.K., Abrishami, M.E., Abd Majid, W.H., Yousefi, R., Hosseini, S.M.: Effects of annealing temperature on some structural and optical properties of ZnO nanoparticles prepared by a modified sol–gel combustion method. *Ceramic Int.* **37**, 393–398 (2011)
54. Mishra, R.R., Prajapati, S., Das, J., Dangar, T.K., Das, N., Thatoi, H.: Reduction of selenite to red elemental selenium by moderately halotolerant *Bacillus megaterium* strains isolated from Bhitarkanika mangrove soil and characterization of reduced product. *Chemosphere* **84**, 1231–1237 (2011)
55. Tiquia-Arashi, S., Rodrigues, D.: Extremophiles: Applications in nanotechnology. Springer, Cham (2017)
56. Azam, A., Ahmed, A.S., Oves, M., Khan, M.S., Memic, A.: Size-dependent antimicrobial properties of CuO nanoparticles against Gram-positive and -negative bacterial strains. *Int. J. Nanomed.* **7**, 3527–3535 (2012)
57. Saeed, M., Ansari, M.T., Kaleem, I., Bajwa, S.Z., Rehman, A., Bano, K., Tehseen, B., Jamil, N., Zahoor, M., Shaheen, A., Taj, A., Younis, M.R., Khan, W.S.: Assessment of antimicrobial features of selenium nanoparticles (SeNPs) using cyclic voltammetric strategy. *J. Nanosci. Nanotechnol.* **19**, 7363–7368 (2019)
58. Vijai Anand, K., Karl Chinnu, M., Mohan Kumar, R., Mohan, R., Jayavel, R.: Formation of zinc sulfide nanoparticles in HMTA matrix. *Appl. Surf. Sci.* **255**, 8879–8882 (2009)
59. Sirikharin, R., Taengchaiyaphum, S., Sanguanrut, P., Thanh, D.C., Mavichak, R., Proespraiwong, P., Nuangsaeng, B., Thitamadee, S., Flegel, T.W., Sritunyalucksana, K.: Characterization and PCR detection of binary, Pir-like toxins from *Vibrio parahaemolyticus* isolates that cause acute hepatopancreatic necrosis disease (AHPND) in shrimp. *PLoS ONE* **10**, e0126987 (2015)
60. Uma Suganya, K.S., Govindaraju, K., Ganesh Kumar, V., Stalin Dhas, T., Karthick, V., Singaravelu, G., Elanchezhian, M.: Blue green alga mediated synthesis of gold nanoparticles and its antibacterial efficacy against Gram positive organisms. *Mater. Sci. Eng. C* **47**, 351–356 (2015)
61. Ansari, M.A., Khan, H.M., Khan, A.A., Ahmad, M.K., Mahdi, A.A., Pal, R., Cameotra, S.S.: Interaction of silver nanoparticles with *Escherichia coli* and their cell envelope biomolecules. *J. Basic Microbiol.* **54**, 905–915 (2014)
62. Stoimenov, P.K., Klinger, R.L., Marchin, G.L., Klabunde, K.J.: Metal oxide nanoparticles as bactericidal agents. *Langmuir* **18**, 6679–6686 (2002)
63. Roy, A., Gauri, S.S., Bhattacharya, M., Bhattacharya, J.: Antimicrobial activity of CaO nanoparticles. *J. Biomed. Nanotechnol.* **9**, 1570–1578 (2013)
64. Geoffrion, L.D., Hesabizadeh, T., Medina-Cruz, D., Kusper, M., Vernet-Crua, P.T.A., Chen, J., Ajo, A., Webster, T.J., Guisbiers, G.: Naked selenium nanoparticles for antibacterial and anticancer treatments. *ACS Omega* **5**, 2660–2669 (2020)
65. Morales-Covarrubias, M.S., Garcia-Aguilar, N., Bolan-Mejia, M.C., Puello-Cruz, A.C.: Evaluation of medicinal plants and colloidal silver efficiency against *Vibrio parahaemolyticus* infection in *Litopenaeus vannamei* cultured at low salinity. *Dis. Aquat. Org.* **122**, 57–65 (2016)
66. Sivaramasamy, E., Zhiwei, W.: Enhancement of vibriosis resistance in *Litopenaeus vannamei* by supplementation of biomastered silver nanoparticles by *Bacillus subtilis*. *J. Nanomed. Nanotechnol.* **7**, 352 (2016)
67. Sivaramasamy, E., Zagorsek, K., Li, F., Xiang, J.: *In situ* synthesis of silver nanoparticles into TEMPO-mediated oxidized bacterial cellulose and their antivibriocidal activity against shrimp pathogens. *Carbohydr. Polym.* **166**, 329–337 (2017)
68. Alvarez-Cirerol, F.J., Lopez-Torres, M.A., Rodriguez-Leon, E., Rodriguez-Beas, C., Martínez-Higuera, A., Lara, H.H., Vergara, S., Arellano-Jimenez, M.J., Larios-Rodriguez, E., Martínez-Porchas, M., Vega, E.R., Iniguez-Palomares, R.A.: Silver nanoparticles synthesized with *Rumex hymenosepalus*: A strategy to combat early mortality syndrome (EMS) in a cultivated white shrimp. *J. Nanomater.* **2019**, 8214675 (2019)
69. Maldonado-Muniz, M., Luna, C., Mendoza-Resendez, R., Barriga-Castro, E.D., Soto-Rodriguez, S., Ricque-Marie, D., Cruz-Suarez, L.E.: Silver nanoparticles against acute hepatopancreatic necrosis disease (AHPND) in shrimp and their depuration kinetics. *J. Appl. Phycol.* **32**, 2431–2445 (2020)
70. Dutta, R., Nenavathu, B.P., Gangishetty, M.K., Reddy, A.: Studies on antibacterial activity of ZnO nanoparticles by ROS induced lipid peroxidation. *Colloids Surf. B* **94**, 143–150 (2012)
71. Xie, Y., He, Y., Irwin, P.L., Jin, T., Shi, X.: Antibacterial activity and mechanism of action of zinc oxide nanoparticles against *Campylobacter jejuni*. *Appl. Environ. Microbiol.* **77**, 2325–2331 (2011)
72. Rotini, A., Tornambe, A., Cossi, R., Iamunno, F., Benvenuto, G., Berducci, M.T., Maggi, C., Thaller, M.C., Cicero, A.M., Manfra, L., Migliore, L.: Salinity-based toxicity of CuO nanoparticles, CuO-bulk and Cu ion to *Vibrio anguillarum*. *Front. Microbiol.* **8**, 2076 (2017)
73. Bogdanovic, U., Lazic, V., Vodnik, V., Budimir, M., Markovic, Z., Dimitrijevic, S.: Copper nanoparticles with high antimicrobial activity. *Mater. Lett.* **128**, 75–78 (2014)
74. Vahdati, M., Moghadam, T.T.: Synthesis and characterization of selenium nanoparticles lysozyme nanohybrid system with synergistic antibacterial properties. *Sci. Rep.* **10**, 510 (2020)

Publisher's Note Springer Nature remains neutral with regard to jurisdictional claims in published maps and institutional affiliations.



Affiliations

D Vinu¹ · K. Govindaraju¹  · R. Vasantharaja¹ · S. Amreen Nisa¹ · M. Kannan² · K. Vijai Anand³

✉ K. Govindaraju
govindarajusu@gmail.com

¹ Centre for Ocean Research (DST-FIST Sponsored Centre),
MoES-Earth Science and Technology Cell, Sathyabama
Institute of Science and Technology, Chennai 600 119, India

² Department of Nano Science and Technology, Tamil Nadu
Agricultural University, Coimbatore 641 003, India

³ Department of Physics, Sathyabama Institute of Science
and Technology, Chennai 600 119, India

